JOURNAL OF THEORETICAL AND APPLIED MECHANICS
41, 1, pp. 119-135, Warsaw 2003

DIFFRACTION LOADS ON MULTIPLE VERTICAL CIRCULAR CYLINDERS BY LEAST-SQUARES TREFFTZ-TYPE FINITE ELEMENTS

Małgorzata Stojek

Department of Computational Methods in Metallurgy, University of Mining and Metallurgy
e-mail: ghstojek@agh.edu.pl

The paper deals with the application of the so-called "frameless" Trefftz-type finite elements to the calculation of wave induced loads on the offshore, seabed, cylindrical structures. The method is based on the use of a suitably truncated T-complete set of Trefftz functions over individual subdomains linked by means of a least square procedure. The Neumann homogeneous boundary conditions and the Sommerfeld radiation condition are readily incorporated in the trial functions of special purpose finite elements.

Key words: Helmholz equation, Trefftz, FEM

1. Introduction

Linearized diffraction theory for vertical cylinders extending from the impermeable seabed to the free surface in water of constant depth leads to the Helmholtz equation in the exterior domain accompanied by the Sommerfeld radiation condition at infinity and the Neumann boundary condition on the wetted cylinder surface. Traditionally, such a problem is reformulated as a boundary integral equation over the surface of the body (Colton and Kress, 1992) giving rise later on to an appropriate variational formulation and a boundary element (BE) approximation. The BE discretization can be done directly on the wetted body or some auxiliary smooth surrounding surface. In the latter case we have the coupling of finite and boundary elements which, although more expensive, avoids problems with the integration of singular kernels arising from BE approximations on non-smooth boundaries (corners, edges).

In both cases mentioned above, the application of the BE approaches turns out expensive for medium and large wave numbers (Harari and Hughes, 1992). An interesting alternative seems to be, therefore, the finite element method with two different approaches to an infinite domain. The first approach introduces an artificial boundary to make the computational domain finite (for overview see Givoli *et al.*, 1997), the second one is based on the use of infinite elements (Bettes, 1992; Gerdes, 1998; Harari *et al.*, 1998). However, the common use of the "traditional" polynomial shape functions results in the so-called pollution error (Babuška and Sauter, 1997) related to the deterioration of stability of the Helmholtz variational form at large wave numbers. To avoid this, several non-standard FE formulations have been proposed in the literature. In these methods, stabilization is either attempted directly by modification of the differential operator or indirectly, via improvement of approximability by the incorporation of particular solutions into the trial space of FEM (for overview see Ihlenburg, 1998; Farhat *et al.*, 2001).

The present paper shows the application of least-squares Trefftz-type elements (Stojek, 1998) to the practical calculations of wave induced loads on the offshore, seabed, cylindrical structures. Such T-elements belong to the non-conforming, knowledge-based finite elements and have been developed directly for the scattering problems and long waves. Their main idea consists in the use of suitably truncated T-complete (Herrera and Sabina, 1978) solutions to the governing differential equation. The prescribed boundary conditions and the interelement continuity are enforced by means of a least-squares procedure. The Neumann homogeneous boundary conditions and the Sommerfeld radiation condition are readily incorporated in the trial functions of special purpose finite elements.

The paper is organized as follows. The next section shortly recalls the theoretical formulation of the least-squares T-type elements. Section 3 summarizes the linear diffraction theory and the wave induced loads on vertical cylinders. Section 4 presents the numerical results for the interference effects among 2, 3 and 4 circular cylinders. Finally, the concluding remarks are given in Section 5.

2. Review of least-squares Trefftz-type finite elements for the Helmholtz equation

We consider the following complex valued boundary problem in 2D (Stojek, 1998)

$$\begin{aligned} &\nabla^2\varphi + k^2\varphi = 0 && \text{in } \Omega \\ &\frac{\partial\varphi}{\partial n} = 0 && \text{on the wetted surface } \Gamma_B \\ &\lim_{r\to\infty}\sqrt{kr}\Big(\frac{\partial\varphi^s}{\partial r} - \mathrm{i}k\varphi^s\Big) = 0 && \text{at infinity } \Gamma_\infty \end{aligned} \tag{2.1}$$

where k is a wavenumber, φ and φ^s denote the two-dimensional unknown total and scattered velocity potentials, respectively, $\varphi^i = \varphi - \varphi^s$ is the given incident potential, Ω stands for the unbounded exterior domain occupied by the fluid, $\Gamma_B \cup \Gamma_\infty = \partial\Omega$, and the boundary condition at infinity is the Sommerfeld radiation condition. We recall that the above physical problem may be formulated both in terms of the total or scattered potentials. In our case, the former is preferred since it leads to the homogeneous boundary conditions on the wetted surface Γ_B.

Let us divide the whole domain Ω into n subdomains Ω_k provided with respective local coordinate systems (r_k, θ_k). Over each Ω_k we represent an approximate solution φ_k as

$$\varphi_k = \varphi^i + \varphi^s_k = \varphi^i + \sum_{j=1}^{m} N_{kj}c_{kj} = \varphi^i + \mathbf{N}_k\mathbf{c}_k \tag{2.2}$$

or

$$\varphi_k = \sum_{j=1}^{m} N_{kj}c_{kj} = \mathbf{N}_k\mathbf{c}_k \tag{2.3}$$

where $\mathbf{N}_k$ is a truncated complete set of local solutions to Helmholtz's equation in Ω_k (so called T-functions) and $\mathbf{c}_k$ denotes a vector of undetermined complex valued coefficients. The corresponding outward normal velocity $v_k = \nabla\varphi_k \cdot \mathbf{n}$ on $\partial\Omega_k$ is

$$v_k = v^i + \mathbf{T}_k\mathbf{c}_k \tag{2.4}$$

or

$$v_k = \mathbf{T}_k\mathbf{c}_k \tag{2.5}$$

The Neumann boundary conditions on Γ_B and the continuity in potential φ and normal derivative v on all subdomain interfaces Γ_I are enforced by minimizing the following least-squares functional

$$I(\varphi) = I(\mathbf{c}) = w^2 \int_{\Gamma_B} |v|^2 \, d\Gamma + \int_{\Gamma_I} |\varphi_I^+ - \varphi_I^-|^2 \, d\Gamma + w^2 \int_{\Gamma_I} |v_I^+ + v_I^-|^2 \, d\Gamma \tag{2.6}$$

where superscripts $+, -$ in the integrals along Γ_I designate the solutions from two respective neighbouring Trefftz fields and w is some positive weight which,

in general, may vary with the segment of matching. Note that the integral along Γ_∞ in (2.6) is not included due to the assumption that the Sommerfeld radiation condition is fulfilled *a priori*.

The vanishing variation of (2.6)

$$\delta I = \delta \mathbf{c}^\dagger \frac{\partial I}{\partial \mathbf{c}} = \delta \mathbf{c}^\dagger \Big(\overset{\circ}{\mathbf{R}} + \mathbf{K}\mathbf{c} \Big) = 0 \tag{2.7}$$

yields for the undetermined coefficients $\mathbf{c}$, of the whole assembly of n subdomains, $\mathbf{c}^\top = [\mathbf{c}_1^\top, \mathbf{c}_2^\top, \mathbf{c}_n^\top]$, the system of linear equations, $\mathbf{K}\mathbf{c} = -\overset{\circ}{\mathbf{R}}$, where $\mathbf{K}$ is Hermitian and positive-definite.

The described approach makes use of the following different types of T-systems, defined in local polar coordinates (r, θ) in terms of the Bessel and Hankel functions, J_n, $H_n^{(1)}$, of the first kind

1. T-functions for the bounded subdomain (Herrera and Sabina, 1978)

$$\Big\{ J_0(kr),\ J_n(kr)\cos n\theta,\ J_n(kr)\sin n\theta \Big\} \tag{2.8}$$

2. T-functions for the unbounded subdomain (Herrera and Sabina, 1978)

$$\Big\{ H_0^{(1)}(kr),\ H_n^{(1)}(kr)\cos n\theta,\ H_n^{(1)}(kr)\sin n\theta \Big\} \tag{2.9}$$

3. Special purpose functions for the doubly connected subdomain with a circular hole

$$\begin{aligned} &\Big\{ \Big(J_0(kr) - \frac{J_0'(kb)}{H_0'(kb)} H_0(kr) \Big),\ \Big(J_n(kr) - \frac{J_n'(kb)}{H_n'(kb)} H_n(kr) \Big) \cos n\theta, \\ &\Big(J_n(kr) - \frac{J_n'(kb)}{H_n'(kb)} H_n(kr) \Big) \sin n\theta \Big\} \end{aligned} \tag{2.10}$$

obtained as the linear combinations of (2.8) and (2.9) fulfilling *a priori* Neumann homogeneous boundary conditions on the circle of radius b (Stojek, 1998).

The T-sets (2.8) and (2.9) approximate the scattered potential in (2.2). They are complete regardless of the specific subdomain considered as long as the condition of being bounded or, alternatively, of being the exterior of a bounded subdomain is fulfilled (Herrera and Sabina, 1978). The T-system (2.10) has been developed directly for the total potential (2.3). Note that the

assumption of the completeness of the T-systems is sufficient for our method to be convergent.

The above systems are non-singular inside the given domain which yields important numerical advantages, i.e. all boundary integrals can be evaluated by means of standard quadrature rules.

3. Wave induced loads on vertical cylinders

We consider an inviscid, incompressible fluid in a constant gravitational field. The space coordinates are denoted by $\mathbf{x}_s = (x, y, z)$ and the gravitational acceleration g is in the negative z direction. Assuming that the flow is irrotational, the incident complex potential of the progressive linear wave in water of constant depth h_0 is known and given by (Mei, 1992)

$$\phi^i = -\frac{\mathrm{i}gH}{2\omega}\frac{\cosh k(z+h_0)}{\cosh kh_0}\mathrm{e}^{\mathrm{i}\mathbf{kx}}$$
$$\mathbf{kx} = k_1 x + k_2 y = kx\cos\alpha + ky\sin\alpha \tag{3.1}$$

where α is the angle of incidence, $\mathbf{k}$ stands for the wavenumber vector, $\omega = \sqrt{gk\tanh kh_0}$ is a frequency and H is the height of the wave.

Let us limit ourselves to an isolated vertical cylinder extending from the seabed and protruding above the free surface. Thus, the incident wave is scattered horizontally and the three-dimensional diffraction problem governed by Laplace's equation may be reduced to two dimensions. Finally, we pose the problem to be solved as follows.

Given the incident potential

$$\varphi^i(x,y) = -\frac{\mathrm{i}gH}{2\omega}\mathrm{e}^{\mathrm{i}k(x\cos\alpha + y\sin\alpha)} \tag{3.2}$$

find the total potential $\varphi(x,y)$ fulfilling two-dimensional problem (2.1). Once the two-dimensional potential φ is found the total velocity potential ϕ may be calculated from

$$\phi(x,y,z) = \varphi(x,y)\frac{\cosh k(z+h_0)}{\cosh kh_0} \tag{3.3}$$

where $\phi(x,y,z)|_{z=0} = \varphi(x,y)$. Then, by integration of the hydrodynamic pressure, $p = i\omega\rho\phi$, over the wetted body surface we obtain the total horizontal force

$$\mathbf{F} = \int_{-h_0}^{0} \mathbf{F}^z \, dz = \int_{-h_0}^{0} dz \int_{\Gamma_B} -p\mathbf{n} \, d\Gamma_B \tag{3.4}$$

We investigate the interference effects among neighbouring vertical cylinders by means of the force ratio R. We define it as the force amplitude on one member of the system, $|\mathbf{F}_i|$, compared to that predicted for an isolated cylinder, $|\mathbf{F}_0|$, under the corresponding wave conditions (the same kb)

$$R = \frac{|\mathbf{F}_i|}{|\mathbf{F}_0|} \tag{3.5}$$

4. Numerical studies

In this section, the interference effects among neighbouring vertical circular cylinders of the same radius b are presented. Since the wave induced loads depend not only on the diffraction parameter kb, and the angle of incidence α, but as well are influenced by the relative geometry of cylinders, the force ratio (3.5) dependence

$$R = f\Big(kb, \frac{L}{b}, \alpha\Big) \tag{4.1}$$

is investigated, where L is the distance between cylinder centers. In what follows, the different configurations of cylinders are examined and the results for the force, in the direction of the incident wave, are summarized in comparison with those generated by the program INTACT (the property of Technische Universität Hamburg-Harburg) based on the generalization of an exact algebraic method for interactions among multiple bodies in water waves (Kagemoto and Yue, 1986).

4.1. Pair of cylinders

Let us now consider the case of two neighbouring cylinders (Fig. 1) exposed to the action of the incident wave with the following parameters

$$\begin{aligned} &H = 1 && \text{(height of the incident wave)} \\ &k \in (0.02, 2) && \text{(range of the wavenumber)} \\ &\Delta k = 0.02 && \text{(increment in the wavenumber)} \\ &\alpha = 0^\circ && \text{(angle of incidence)} \end{aligned} \tag{4.2}$$

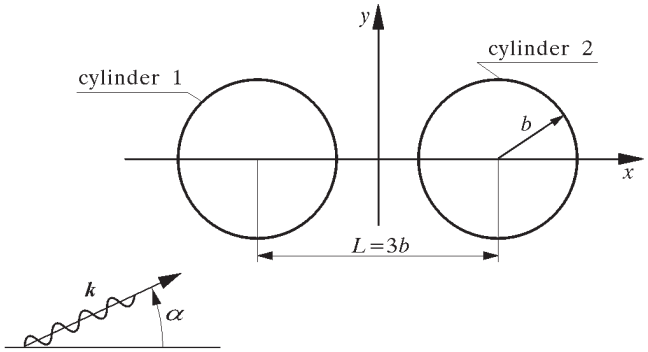

Fig. 1. Scattering of the incident wave by two vertical, circular cylinders. Problem definition

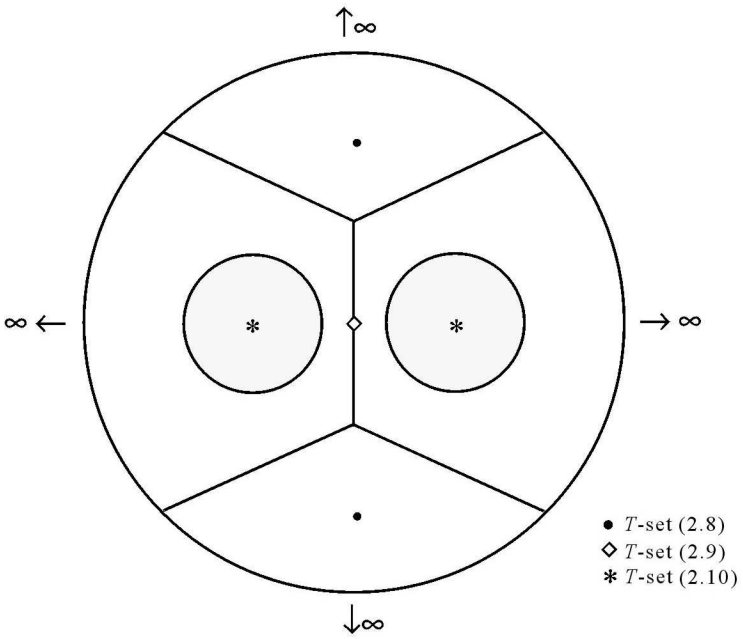

Fig. 2. Subdomain subdivision for two vertical, circular cylinders of Fig. 1. Markers stand for the origins of local coordinate systems

The radius of each cylinder b is equal to one. The T-fields subdivision, with $m = 41$ T-functions per subdomain, is shown in Fig. 2. Here, the use is made of three different T-sets, namely,

- (2.8) in 2 bounded subdomains,

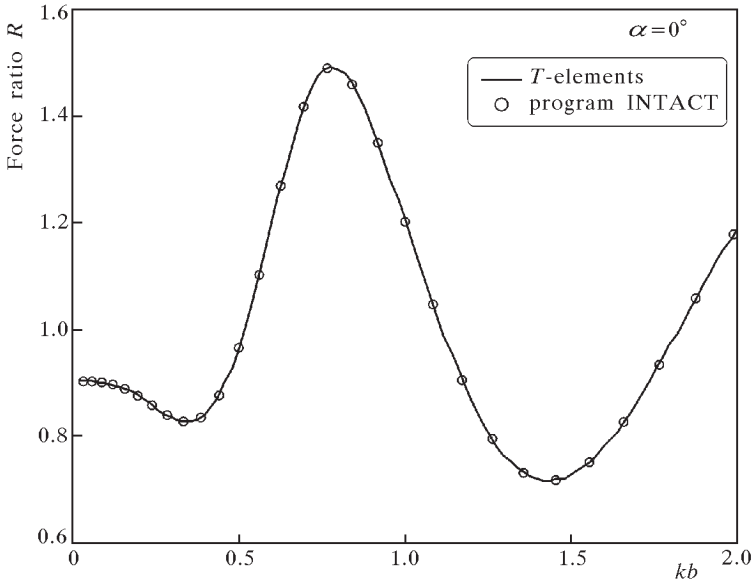

Fig. 3. Interference between the circular cylinders (Fig. 1) shown as the force ratio (4.1) for the first cylinder versus the diffraction parameter kb. Mesh Fig. 2, number of T-functions $m = 41$, reference solution-program INTACT

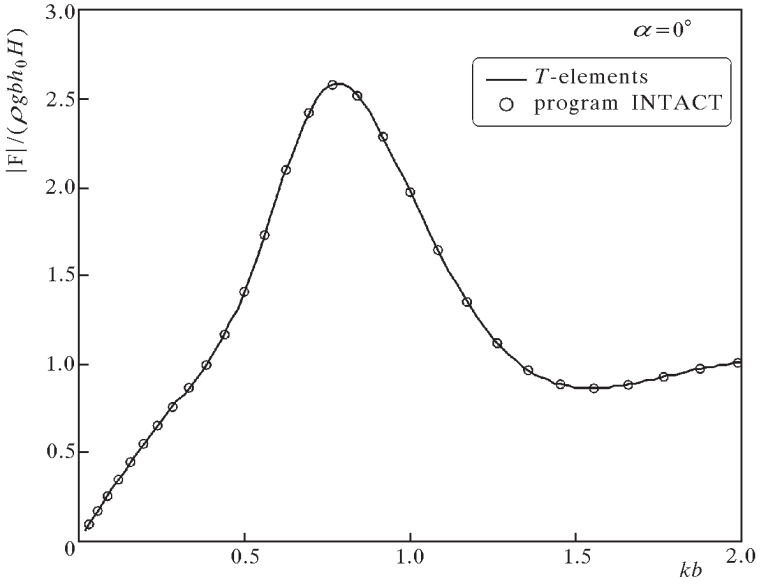

Fig. 4. Interference between the circular cylinders (Fig. 1). Amplitude of the nondimensional force on the first cylinder versus the diffraction parameter kb. Mesh Fig. 2, number of T-functions $m = 41$, reference solution-program INTACT

- (2.9) in the unbounded subdomain,
- (2.10) in 2 doubly connected subdomains with a circular hole.

The results of numerical studies are summarized in Fig. 3, where the force ratio (4.1) is plotted versus the diffraction parameter kb. A comparison of the numerical predictions and the experimental results is presented in Isaacson (1979). Finally, the amplitude of the nondimensional force on the first cylinder for the entire, chosen range of kb is shown in Fig. 4.

4.2. Three cylinders in a row

Let us now focus our attention on three identical cylinders in a row (Fig. 5). This time, the parameters for the incident wave are assumed as follows

$$\begin{aligned} &H = 1 && \text{(height of incident wave)} \\ &k \in (0.02, 2.5) && \text{(range of wavenumber)} \\ &\Delta k = 0.02 && \text{(increment in wavenumber)} \\ &\alpha = 0^\circ, 30^\circ, 60^\circ && \text{(angle of incidence)} \end{aligned} \tag{4.3}$$

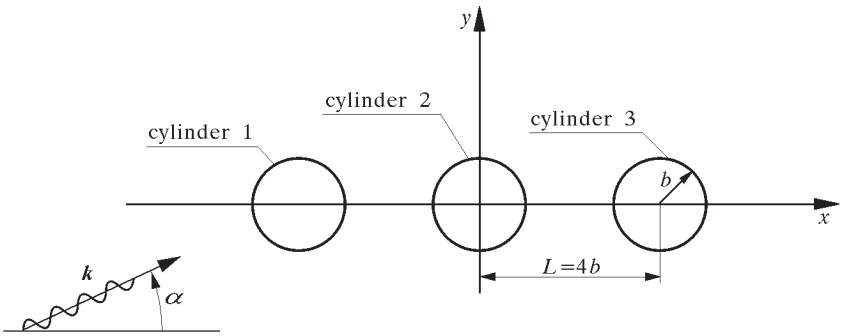

Fig. 5. Scattering of the incident wave by three vertical, circular cylinders in a row. Problem definition

The radius of each cylinder b is again equal to one, but the distance between two neighbouring cylinder centers is increased to $L = 4b$. The subdivision into one unbounded and 15 bounded T-fields is presented in Fig. 6. Note that the use of the three doubly connected subdomains, each equipped with special purpose functions (2.10) for a circular hole, is essential for this subdomain mesh. The number m of T-functions over one subdomain is taken to be $m = 41$.

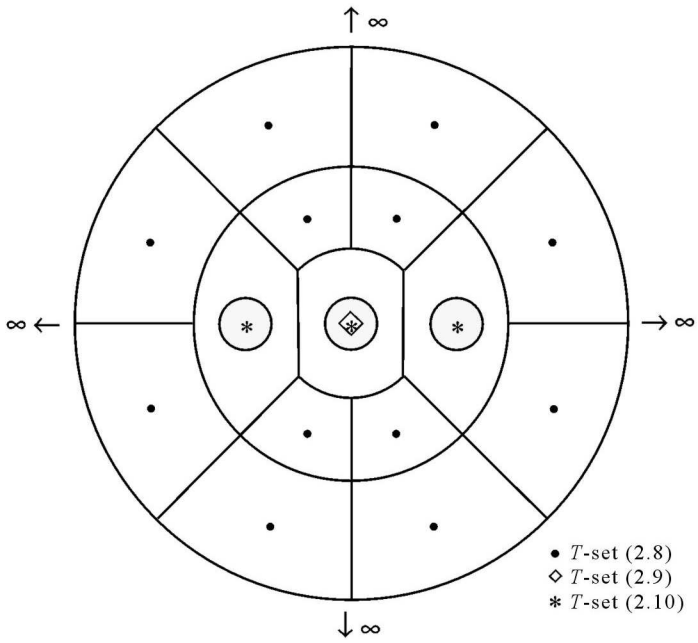

Fig. 6. Subdomain subdivision for three vertical, circular cylinders in a row (Fig. 5). Markers stand for the origins of local coordinate systems

The numerical results for the interference effects are presented for the three cylinders in the following way:

- force ratio (4.1) versus the diffraction parameter kb for $\alpha = 0°$ in Fig. 7,
- amplitude of the nondimensional force on the first cylinder versus the diffraction parameter kb for different α (Fig. 8).

One can observe that the first cylinder in a row is the most affected by the interference of the waves. Nevertheless, in the case of $\alpha = 0°$, the maximal force ratio R for the cylinder in the middle is very close in value to that for the first cylinder (Fig. 7).

4.3. Four cylinders

In this section, the interference effects for four cylinders (Fig. 9) are investigated. The respective T-fields subdivision, consisting of one unbounded subdomain with T-set (2.9) and four doubly connected subdomains provided with special purpose functions (2.10) for a circular hole, is given in Fig. 10. The number m of T-functions over each subdomain is 41. The height of the

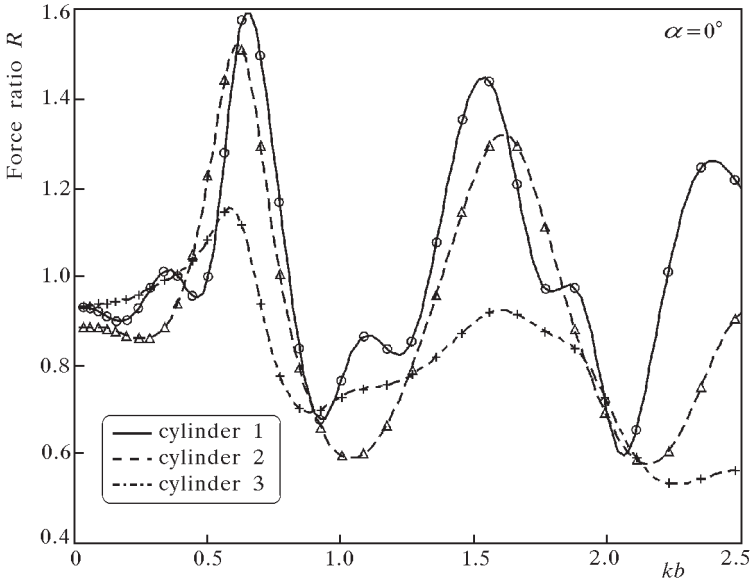

Fig. 7. Interference among three circular cylinders in a row (Fig. 5). Mesh Fig. 6, number of T-functions $m = 41$, markers indicate the solutions obtained by program INTACT

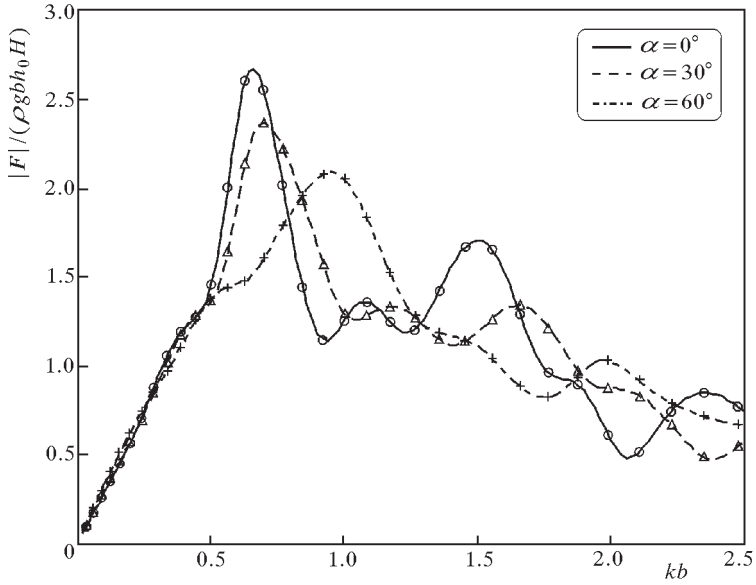

Fig. 8. Interference among three circular cylinders in a row (Fig. 5). Amplitude of the nondimensional force on the first cylinder versus the diffraction parameter kb. Mesh Fig. 6, number of T-functions $m = 41$, markers indicate the solutions obtained by program INTACT

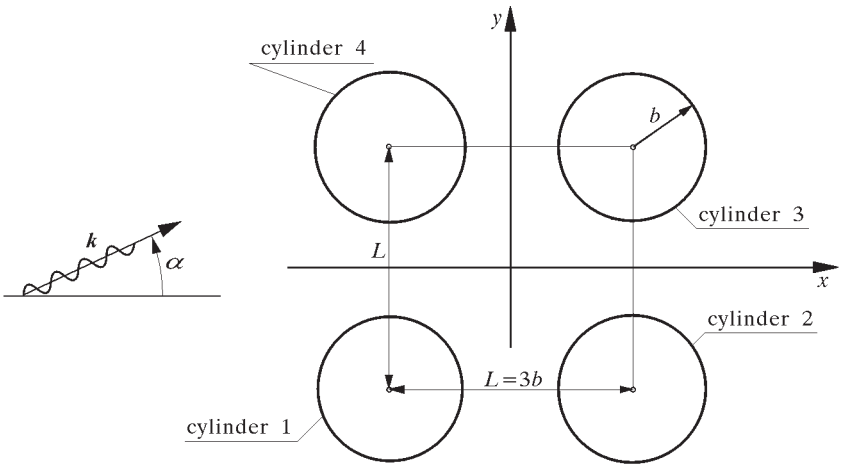

Fig. 9. Scattering of the incident wave by four vertical, circular cylinders. Problem definition

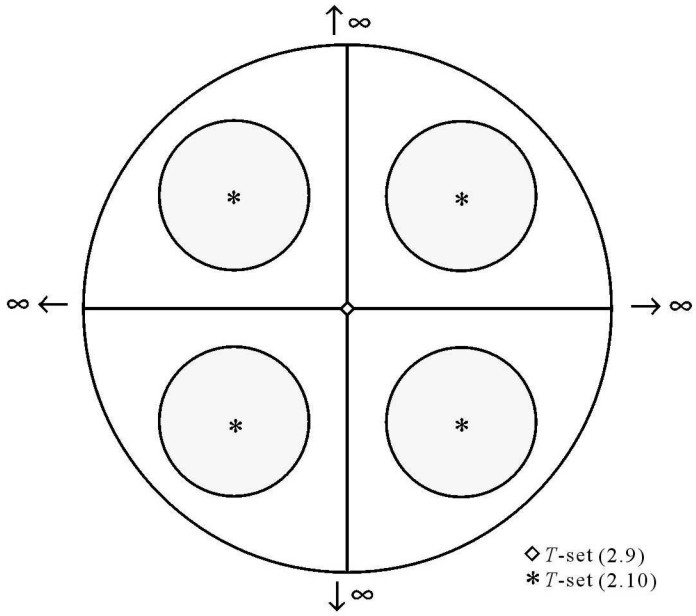

Fig. 10. Subdomain subdivision for four vertical, circular cylinders of Fig. 9. Markers stand for the origins of local coordinate systems

incident wave H is equal to one, and the range of the wavenumber is increased to 5, namely $k \in (0.02, 5)$. The increment in the wavenumber for the most of the range is taken to be $\Delta k = 0.02$, only when a denser approximation is required, is the step reduced to 0.001.

First, the incident wave propagating in the x Cartesian coordinate direction ($\alpha = 0°$) is examined. The results for force ratio (4.1) versus the diffraction parameter kb are displayed in Fig. 11. Next, the angle of incidence $\alpha = 45°$ is considered and the force ratio R versus the diffraction parameter kb is plotted in Fig. 12. Here, one can observe that for the first and third cylinder the force ratio R is much greater in the vicinity of $kb = 2.76$ than away from the "resonance". The details for the range $k \in (2.5, 3)$ are given in Fig. 13. Finally, the amplitude of the nondimensional force on the first cylinder versus the diffraction parameter kb for $\alpha = 45°$ is shown in Fig. 14.

5. Concluding remarks

The application of the so-called least-squares T-elements to the calculation of the diffraction loads on the multiple vertical cylinders with circular cross sections in waves has been presented. Such an approach has led to sufficiently accurate solutions for only few subdomain divisions due to the fact that the oscillatory nature of the wave is inherent in all kinds of Bessel's functions, and as a consequence, in contrast to a polynomial approximation, the dimension of the T-subdomain need not be related in any way to the wavelength. We also recall that the T-type approach has the benefit of *a priori* satisfaction of the radiation condition at infinity, though, special methods developed for infinite domains are not needed.

In addition, the use of the special purpose functions for the doubly connected subdomain has resulted in the quick convergence and good accuracy for amplitudes and phases of the calculated forces on the wetted surfaces. It should also be recalled that for applications in offshore engineering, the most important issue is the accuracy of the results on the wetted surface. Thus, one can suppose, that the best approximate solution should fulfill optimally the relevant boundary conditions. Indeed, the presented approach manifests such a property.

The computational results showed the influence of the neighbouring bodies on the diffraction forces. The force amplification factor obtained for the array of cylinders and $\alpha = 45°$ in the "resonance range" was almost 5 which showed the importance of the effects of wave trapping in the interior of the array.

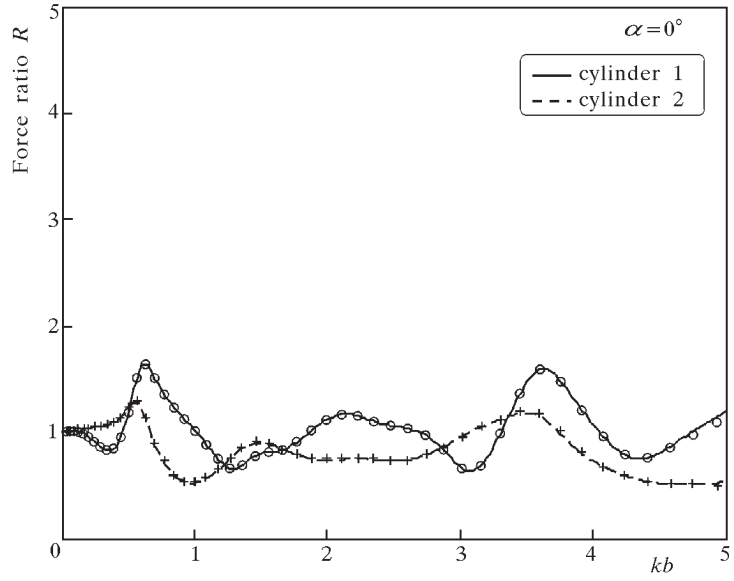

Fig. 11. Interference among four circular cylinders (Fig. 9). Mesh Fig. 10, number of T-functions $m = 41$, markers indicate the solutions obtained by program INTACT

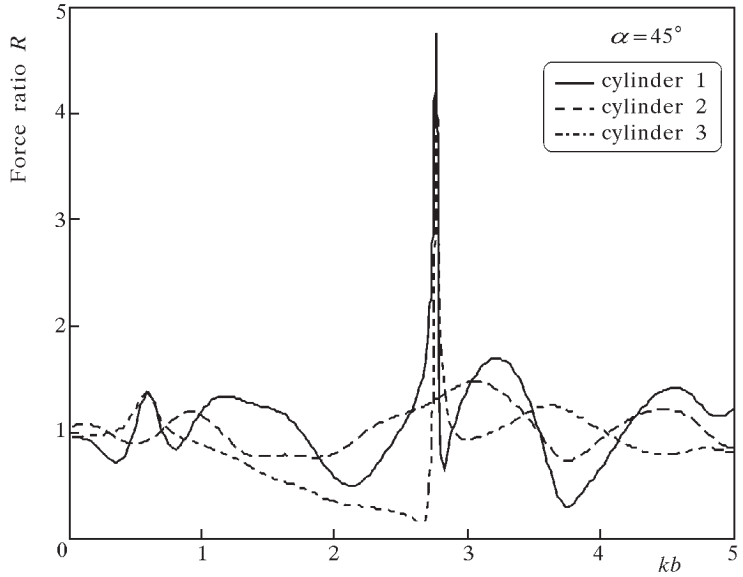

Fig. 12. Interference among four circular cylinders (Fig. 9). Mesh Fig. 10, number of T-functions $m = 41$

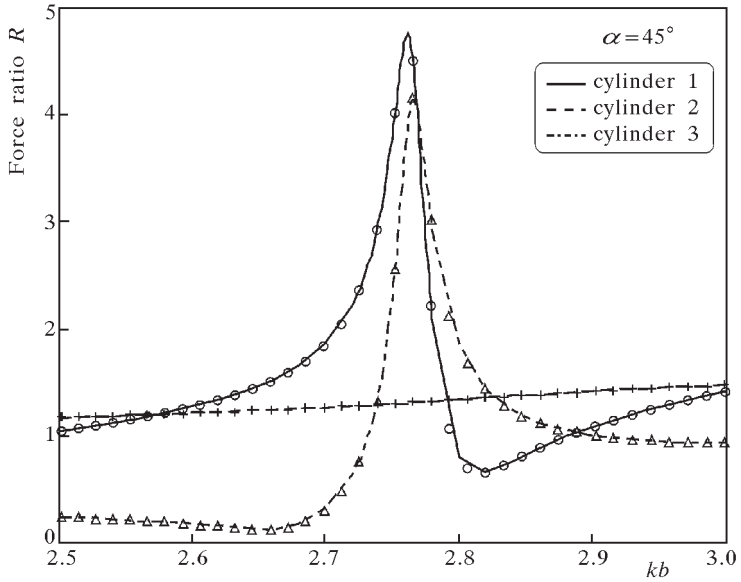

Fig. 13. The "resonance" range for the interference among four circular cylinders (Fig. 9). Mesh Fig. 10, number of T-functions $m = 41$, markers indicate solutions obtained by program INTACT

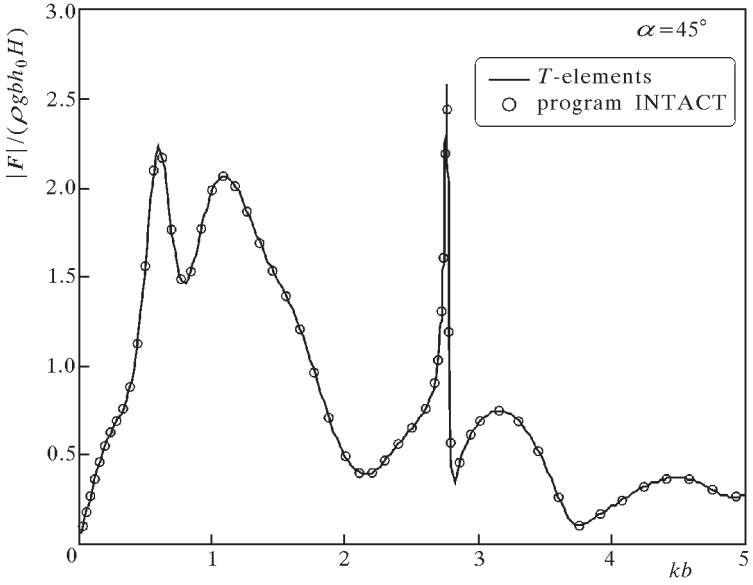

Fig. 14. Interference among four circular cylinders (Fig. 9). Amplitude of the nondimensional force on the first cylinder versus the diffraction parameter kb. Mesh Fig. 10, number of T-functions $m = 41$, reference solution-program INTACT

References

1. Babuška I., Sauter S.A., 1997, Is the pollution effect of the FEM avoidable for the Helmholtz equation considering high wave numbers? *SIAM J. Numer. Anal.*, **34**, 2392-2423

2. Bettes P., 1992, *Infinite Elements*, Penshaw Press, Sunderland

3. Colton D., Kress R., 1992, *Integral Equation Methods in Scattering Theory*, Wiley, New York

4. Farhat C., Harari I., Franca LP., 2001, The discontinuous enrichment method, *Comput. Methods Appl. Mech. Engng.*, **190**, 6455-6479

5. Gerdes K., 1998, A summary of infinite element formulations for exterior Helmholtz problems, *Comput. Methods Appl. Mech. Engng.*, **164**, 95-105

6. Givoli D., Patlashenko I., Keller J.B., 1997, High-order boundary conditions and finite elements for infinite domains, *Comput. Methods Appl. Mech. Engng.*, **143**, 13-39

7. Harari I., Barbone P.E., Slavutin M., Shalom R., 1998, Boundary infinite elements for the Helmholtz equation in exterior domains, *Int. J. Numer. Meth. Engng*, **41**, 1105-1131

8. Harari I., Hughes T.J.R., 1992, A cost comparison of boundary element and finite element methods for problems of time-harmonic structural acoustics, *Comput. Methods Appl. Mech. Engng.*, **97**, 77-102

9. Herrera I., Sabina F.J., 1978, Connectivity as an alternative to boundary integral equations: Construction of bases, *Proc. Nat. Acad. Sci. USA*, **75**, 2059-2063

10. Ihlenburg F., 1998, *Finite Element Analysis of Acoustic Scattering*, Springer

11. Isaacson M. de St. Q., 1979, Interference effects between large cylinders in waves, *J. Petroleum Tech.*, **31**, 4, 505-512

12. Kagemoto H., Yue D.K.P., 1986, Interaction among multiple three-dimensional bodies in water waves: an exact algebraic method, *J. Fluid Mech.*, **166**, 189-209

13. Mei C.C., 1992, *The Applied Dynamics of Ocean Surface Waves*, World Scientific, Singapore

14. Stojek M., 1998, Least-squares Trefftz-type elements for the Helmholtz equation, *Int. J. Numer. Meth. Engng*, **41**, 831-849

Obciążenia dyfrakcyjne fal wodnych na układy pionowych cylindrów o przekroju kołowym za pomocą elementów skończonych "typu Trefftza"

Streszczenie

Artykuł prezentuje zastosowanie elementów skończonych "typu Trefftza" do obliczeń obciążeń dyfrakcyjnych fal wodnych na układy pionowych cylindrów o przekroju kołowym. Metoda jest oparta na aproksymacji rozwiązań w podobszarach za pomocą skończonej sumy szeregu funkcji "T-zupełnych" (funkcji kształtu). Rozwiązanie globalne jest otrzymane przez "zszycie" rozwiązań lokalnych i wymuszenie warunków brzegowych za pomocą metody najmniejszych kwadratów. Jednorodne warunki brzegowe Neumanna i warunek radiacyjny Sommerfelda są zawarte w specjalnych elementach skończonych.

Manuscript received May 6, 2002; accepted for print October 8, 2002